Landmarks in Earth Reinforcement, Ochiai et al. (eds),
© 2001 Swets & Zeitlinger, ISBN 90 2651 863 3

Seismic ductility of cut slope reinforced by soil nail

A. Takahashi, J. Izawa & O. Kusakabe
Tokyo Institute of Technology, Tokyo, Japan

S. Tayama & M. Takemoto
Expressway Research Institute, Japan Highway Public Corporation, Tokyo, Japan

ABSTRACT: This paper describes an experimental study on seismic ductility of cut slope reinforced by soil nail using a geotechnical centrifuge. Effects of length and diameter of the soil nails on the permanent deformation of the cut slopes were discussed in terms of the ductility of the reinforced slopes.

1 INTRODUCTION

Soil nail reinforcement has been widely applied to steep cut slopes, particularly for expressway constructions (Tayama & Kawai, 1999). Most of the existing design methods for the soil nail reinforced slopes are based on empirical methods and/or the limit equilibrium analyses (JH, 1998), neglecting the ductility of the reinforced soil structure against deformation. In this study, pullout tests for a model soil nail and centrifuge model tests were conducted to evaluate the ductility of reinforced cut slopes during earthquakes. Effects of length and diameter of the soil nails on the permanent deformation of the slopes were also discussed.

2 TEST PROCEDURE AND CONDITIONS

2.1 *Test procedure*

Geogechnical centrifuge used in the tests was T.I. Tech Mark II Centrifuge (Takemura et al. 1989). Model set-up used is shown in Fig.l. DL clay was used for making the model ground. Material properties of DL clay are given in Table 1. Friction angle, ϕ was obtained from the triaxial compression tests under drained conditions and was modified considering the plain strain condition in the centrifuge tests. Cohesion, c was back calculated from the failure height observed in a centrifuge test on non-reinforced vertical slope.

An aluminium model container with inner sizes of 450mm in width; 150mm in breadth and 250mm in height was used. Rubber sheets were placed at both side of the container for absorbing of stress waves from the side boundaries. DL clay with water content of 20% was statically compacted to the bulk density $\rho_t = 1.4 Mg/m^3$ layer-by-layer using a bellofram cylinder. This compaction was continued up to the top level of the model slope. After completion of soil compaction, templates were placed and the compacted soil was formed into the slope shape. Model soil nails, which were 0.58mm diameter nickel spiral guitar strings, were installed into drilled holes on the slope surface with glue or plaster made grout material arranged in gridiron at intervals of 30mm, which is equivalent to 1.5m in the prototype scale. The arrangement of the soil nails for the tests are shown in Fig.2. In order to avoid the local failure at the face of the slope, transparent sheet made facing plate was adopted.

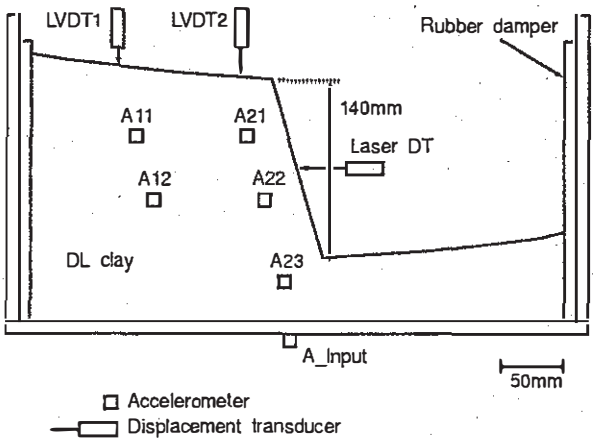

Figure 1. Model set-up for centrifuge test.

Table 1. Material properties of DL clay.

Specific gravity	2.68
Mean grain size D_{50}	$0.024mm$
Maximum void ratio	1.672
Minimum void ratio	0.695
Cohesion c*	$9.2kPa$
Internal friction angle ϕ*	$40.5deg.$

* $\rho_t = 1.4 Mg/m^3$, w = 20%

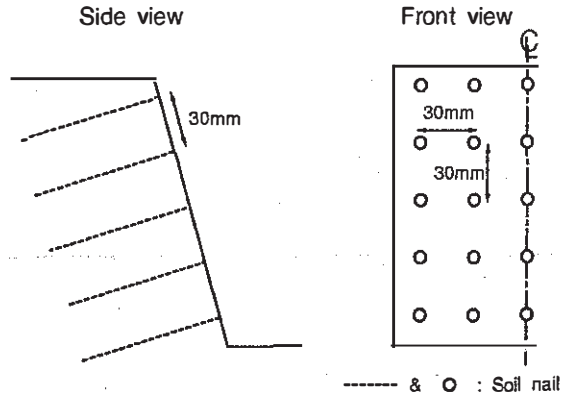

Figure 2. Soil nail arrangement.

Table 2. Applied sinusoidal waves in the test.

Wave	Nominal amplitude (G)	Frequency (Hz)	Number of waves
1st	10 (0.2)	100 (2)	20
2nd	15 (0.3)	100 (2)	20
3rd	20 (0.4)	100 (2)	20
4th	20 (0.4)	100 (2)	40

In parentheses, prototype scale

Table 3. Test conditions.

Case	Slope ascent	L (mm)	D (mm)	Facing plate
1	1:0.5 (63°)	-	-	No
2	1:0.4 (68°)	-	-	No
3*	1:0.3 (73°)	-	-	No
4	1:0.3 (73°)	80	2	No
5	1:0.3 (73°)	80	2	Yes
6	1:0.3 (73°)	80	7	Yes
7	1:0.3 (73°)	40	7	Yes

* Failed at 45-G centrifugal acceleration

Having prepared the model, the container was set on the shaking table mounted on the centrifuge. Shaking tests were conducted under 50-G centrifugal acceleration by sinusoidal waves with a frequency of 100Hz, which is equivalent to 2Hz in the prototype, to the shaking table. Four waves with different conditions as shown in Table 2 were input to each model. Typical time histories of the input sinusoidal waves in the prototype scale are shown in Fig.3. During shaking, acceleration and displacement of the reinforced soil were measured at the locations shown in Fig.1. Photographs were taken before and after shaking to observe the displacements of targets on the front surface of the reinforced soil.

2.2 *Test conditions*

Table 3 gives the test conditions adopted in this study. Height of the cut slope wall was 140mm, which corresponds to 7m in the prototype scale. Effects of the facing plate, the diameter (D) of drilled holes for the soil nails and length (L) of the soil nails on the permanent deformation were investigated. In

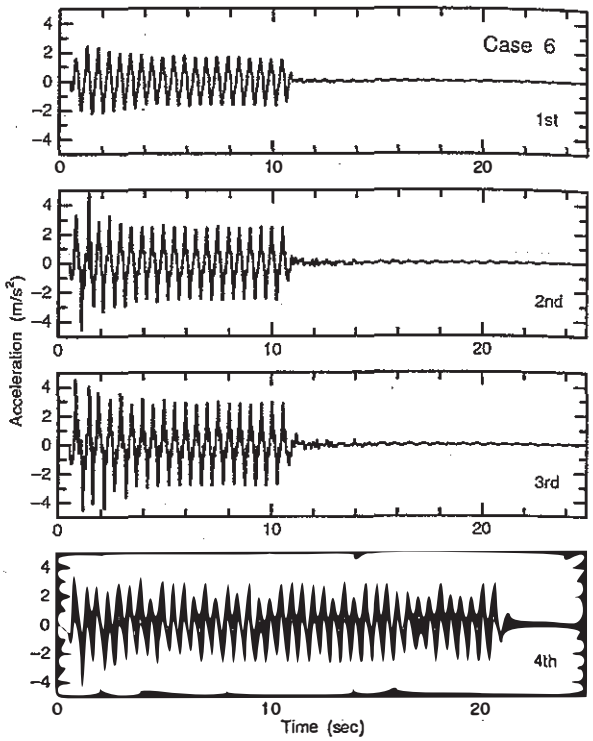

Figure 3. Input waves acceleration time histories (Case 6).

Cases 1-3, no reinforcements were applied. In Case 3, as the brittle failure of the slope took place when the centrifugal acceleration reached 45-G during the spinning up of the centrifuge, whose slope ascent was 73°, no data were available for this particular case.

3 TEST RESULTS AND DISCUSSION

All centrifuge test results presented in this section are in the prototype scale.

3.1 *Pull-out tests on soil nail*

To investigate frictional interaction between the DL clay and the model soil nail, pullout tests were conducted using a small pullout test apparatus. As the diameter (D) of drilled holes for the soil nails was varied in the centrifuge tests, the pullout tests for two sizes of the hole were carried out under different two overburden pressures as listed in Table 4. Typical test results of the pullout test for the overburden pressure of 39.2kPa are shown in Fig.4. The pullout resistance τ shown in the figure is defined as $\tau = F/\pi DL$, where F is a pullout force, D is the diameter of the drilled hole and L is the length of the nail in soil. Ratios R_p of the peak pullout resistance (τ at peak) to the soil strength ($= c + \sigma'_v \tan \phi$) of the DL clay were obtained as shown in Table 4, where σ'_v is the overburden pressure, c and ϕ are the strength parameters of the DL clay.

Though, at the beginning of the pulling, the slope of the relationship between the mobilised pullout resistance and the pullout length was almost the same for the same overburden pressure, the peak pullout resistance of the nail and the pullout lengths of the nails, when the frictional resistance was fully mobilised, were heavily affected by types of the grout materials and the diameters of the drilled hole. In the cases with the small diameter of the drilled hole, the relative displacements between the soil nails and the grouting were observed. It seemed that these were attributed to lack in the grouting itself and adhesion between the nail and the grouting, and they result in the low pullout resistance.

Table 4. Pull out test conditions and results.

Case	D·mm	Grout material	Overburden pressure(kPa)	R_p
1	2	glue	39.2	0.15
2	2	glue	78.4	
3	7	plaster	39.2	0.42
4	7	plaster	78.4	

R_p: Ratio of peak pullout resistance to soil strength

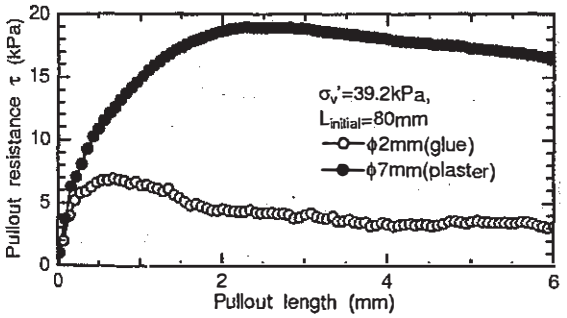

Figure 4. Typical pullout test results for $\sigma'_v = 39.2kPa$.

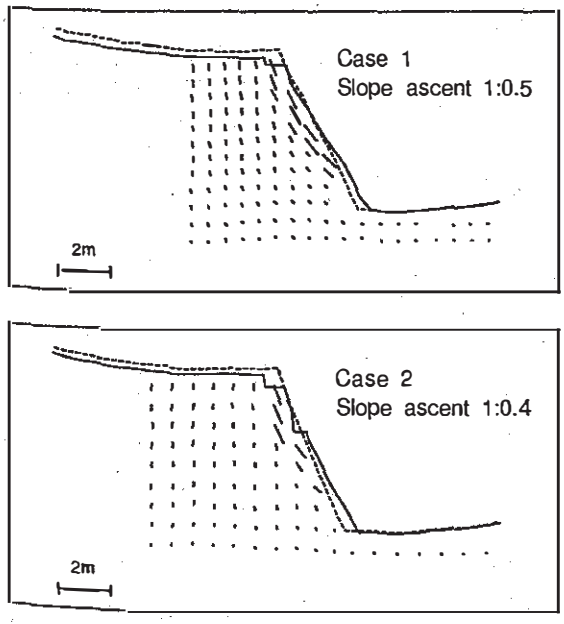

Figure 5. Permanent deformation of the cut slope (just after the third shaking in Cases 1 &2).

3.2 *Failure of the non-reinforced cut slope in centrifuge tests*

Observed permanent deformations for the non-reinforced cut slopes, Cases 1 & 2, just after the third shaking step are shown in Fig. 5. Figure 6 shows the time histories of the settlement at the slope shoulder for Cases 1 & 2 in the first and third shaking steps. In both cases, settlements increased gradually in the first step, while drastic large settlements occurred in the third step. In the third step, slip surfaces appeared at the shallow portion from the slope surfaces as shown in the figure. In Case 3, the brittle failure of the slope took place when the centrifugal acceleration reached 45-G during the spinning up of the centrifuge.

3.3 *Deformation progress of the reinforced cut slope*

Observed permanent deformation of the reinforced cut slope in Cases 4 & 5 are shown in Fig.7. The slopes were reinforced with the nails installed into the 100 mm diameter drilled holes in these cases. Considering the fact that the slope ascent of 73° is not self-supportable without reinforcement as mentioned in Section 2.2, the soil nail reinforcement shows its efficiency to the stabilization of the cut slope. During the shaking, slip surfaces appeared as shown in the figure. Although the slip surfaces were

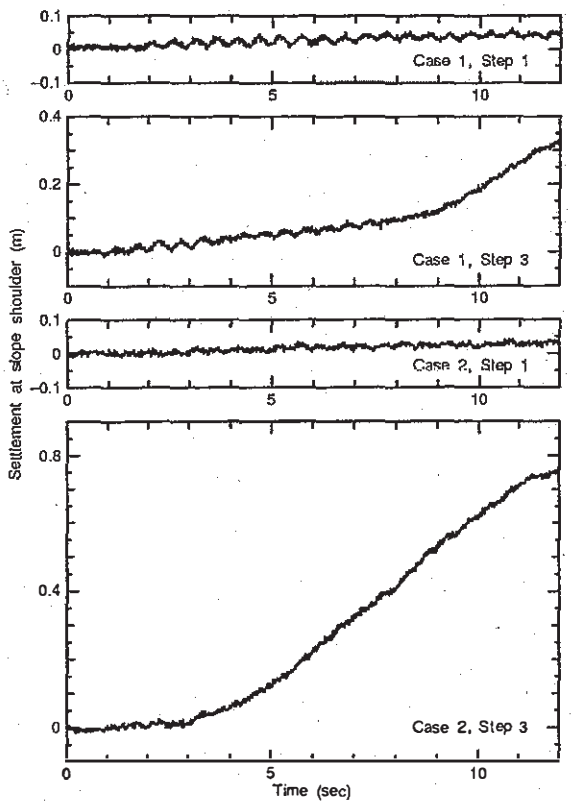

Figure 6. Time histories of the settlement at the shoulder for the first and third step in Cases 1 & 2.

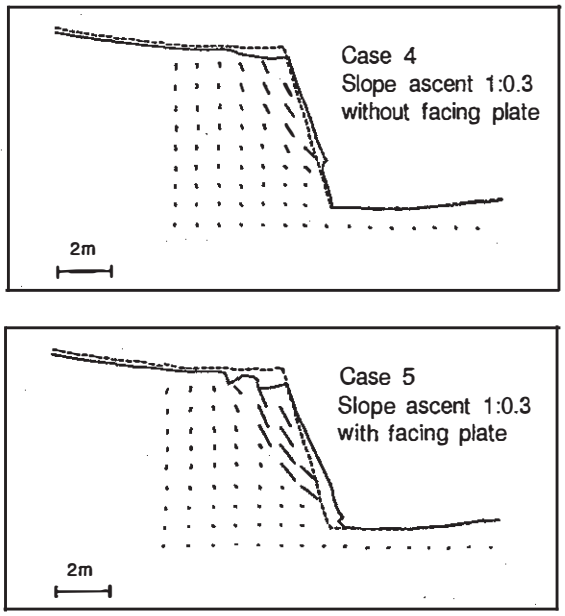

Figure 7. Permanent deformation of the cut slope (just after the second shaking in Cases 4 &5).

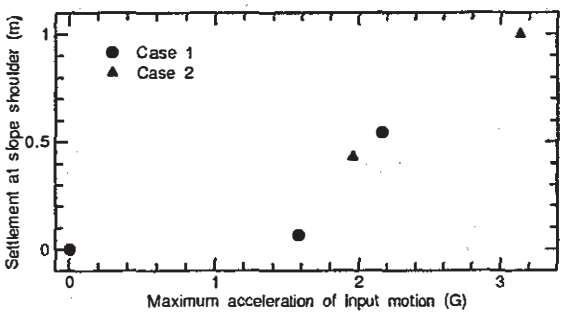

Figure 8. Settlement at the shoulder against maximum acceleration of the input motion (Cases 4 &5).

observed in the reinforced zones, the slip surfaces appeared in deeper portions, compared to the non-reinforced slope. In the other reinforced slope cases with the large diameter of the drilled holes for nailing, Cases 6 & 7, no failure of the slope was observed even after the forth shaking step.

Comparing Cases 4 & 5 from the viewpoint of the effectiveness of the facing plate on the prevention of the local failure, the slip surface passed trough the slope face when the facing plate was not adopted while it passed the slope toe with the plate. Total settlements of the slope shoulder are plotted against to the maximum acceleration of the input motion in Fig.8. Unique relationship between the settlement and the input motion acceleration can be seen in the figure. According to this figure, the effect of the existence of the face plate on the total deformation of the slope was not remarkable in this study, as the facing plates were very thin and had a low flexural rigidity.

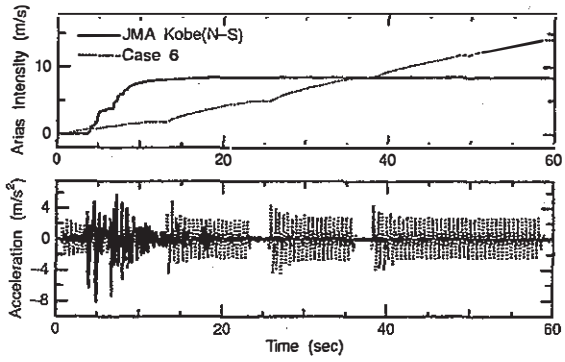

Figure 9. Time histories of acceleration record and Arias intensity.

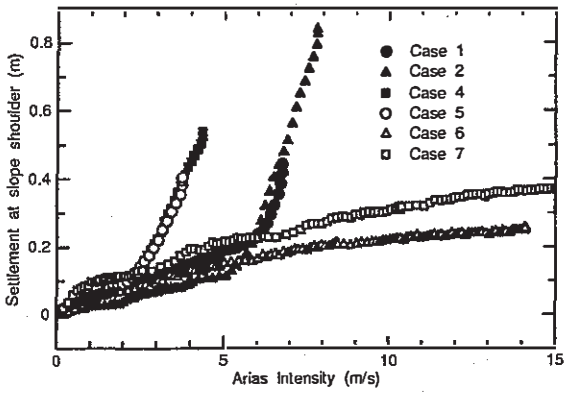

Figure 10. Variations of the settlement at the shoulder against Arias intensity.

To gain insight into the ductility of the reinforced slope during earthquakes, the relationships between the permanent displacement of the slopes and the intensity of earthquakes were examined. As one of the indices for the intensity of earthquake, Arias intensity was introduced (Arias, 1970, Kayen & Mitchell, 1997). This index, I_a is defined as

$$I_a(t) = \frac{\pi}{2g}\int_0^t a^2(\tau)d\tau,$$

where g is gravitational acceleration and $a(t)$ is the acceleration of the input motion at time t. This intensity represents some sort of a dissipated energy per unit weight of soil. Variation of I_a with time for Case 6 and the actual earthquake record at Kobe Marine Observatory in 1995 Hyogoken-Nambu Earthquake are plotted in Fig.9. In this study, very large intensity of the earthquake motions was assumed as shown in the figure.

Figure 10 shows the variations of the settlement at the slope shoulder against Arias intensity for all the cases. Cases 1, 2, 4 & 5 show drastic increase of the settlement and result in failure during earthquake. Meanwhile, in Cases 6 & 7, the settlements level off and shake down against the earthquake intensity. From this figure, the relationships can be

classified into two types. These two typical types of the relation are shown in Fig.11. In the former type, the relationship can be simplified into bi-linear and divided into two phases, Phase I & II, as shown in the upper figure of Fig. 11:

Phase I: The settlement gradually increases with Arial intensity. No localisation of deformation can be observed in the slope.

Phase II: The settlement shows a drastic increase resulting in catastrophic failure. The deformation is localised and the slip surface appears.

In the latter type, Cases 6 & 7, shown in the lower figure of Fig.ll, as the excessive reinforcement was adopted, no localisation of deformation, i.e., no transition to Phase II, was occurred resulting in shaking down. As the localisation of deformation can be observed only in Phase II, a scope of application for deformation analyses of the simplified analysis such as Newmark's sliding block method may be limited in this phase. As the permanent deformation accumulated in Phase I is not negligible, alternative analysis methods, i.e., FE analysis employing a constitutive equation considering dilatancy and compression characteristics of soils under cyclic loading appropriately, should be conducted to estimate the permanent deformation of the slope.

To evaluate the ductility of the cut slope from the test results, the permanent displacements accumulated in Phase I, v_I, were examined. The settlements in Phase I are shown in Fig.12 with the slope ascents. The larger settlement in Phase I may correspond to the higher ductility of the cut slope. The settlement v_I becomes larger as the slope ascent decreases in the cases without reinforcement. Paying attention to the cases with reinforcement, the soil nail reinforcement is very effective in making the ductility of the slope higher, considering the fact that the slope ascent of 73° is not self-supportable without reinforcement.

The increasing rates of the settlements against Arias intensity, $\Delta v/\Delta I_a$, were also examined to evaluate the ductility of the slope. The smaller $\Delta v/\Delta I_a$ may represent the higher ductility of the cut slope. Figure 13 shows the increasing rates of the settlements against Arias intensity for Cases 1, 2, 4 & 5 with the slope ascents. In Phase I, the results were relatively smaller than those in Phase II and the differences were very small. No clear relation can be seen to the slope ascent and the existence of the reinforcement. In the meanwhile, remarkable differences were found in Phase II. Corresponding to the slope ascent, $\Delta v/\Delta I_a$ for Case 1 was smaller than that for Case 2. The increasing ratios for Cases 4 & 5 were also smaller than that for Case 2. The effectiveness of the soil nailing on the ductility of the slope can be reconfirmed by these results.

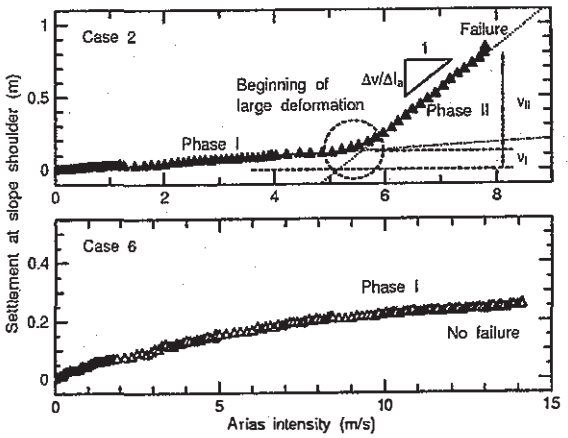

Figure 11. Typical variations of the settlement at the shoulder against Arias intensity.

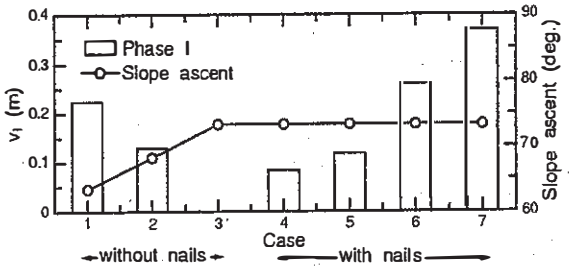

Figure 12. Settlement in Phase I.

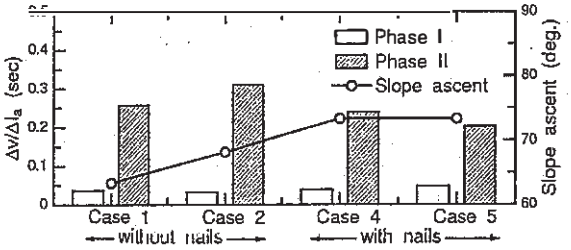

Figure 13. Increasing rates of the settlements against Arias intensity in Phase I & II.

4 CONCLUSIONS

In this study, centrifuge tests were carried out to investigate the effects of the length and the diameter of the soil nailing on the ductility of the reinforced cut slope during earthquakes. Following conclusions are drawn;

(1) The cut slope without any reinforcement shows the brittle failure during the ground motion, while the permanent displacements gradually increased when the soil nail reinforcement was adopted.

(2) The slope reinforced with poor grouted nailing exhibited the slip surface during earthquake. Although the slip surfaces were observed in the re-

inforced zones in these particular cases, the slip surfaces appeared in deeper portions, compared to the non-reinforced slopes.

(3) Arias intensity was used to examine the relationship between the permanent deformation of the cut slope and the earthquake intensity. The beginning of the localisation of the slope deformation can be clarified by this relation obtained from the tests results.

(4) The ductility of the soil nail reinforced cut slope was qualitatively assessed by the settlement before the appearance of the slip surface and the increasing rate of the slope shoulder settlement against Arias intensity.

REFERENCES

Tayama, S. & Kawai, Y. 1999. The current status and outlook for soil nailing in Japan. *Earth reinforcement technique in Asia, Special Volume for the Proc. of ARCSMGE,* 51-61.

Japan Highway Public Corporation. 1998. Design and construction manual for reinforced cut slope (in Japanese.)

Takemura, J., Kimura, T., & Suemasa, N. 1989. Development of Earthquake simulators at Tokyo Institute of Technology. *Technical Report, Dept. Civil Engrg. Tokyo Institute of Technology,* No. 40, 41-60.

Arias, A. 1970. A measure of earthquake intensity. *Seismic design for nuclear power plants,* Hansen, R.J. ed., MIT Press.

Kayen, R.E. & Mitchell, J.K. 1997. Assessment of liquefaction potential during earthquakees by Arias intensity. *J. Geotech. and Geoinvir. Engrg.,* ASCE, 123(12), 1162-1174.